

Lung inhomogeneities and time course of Ventilator-Induced mechanical injuries

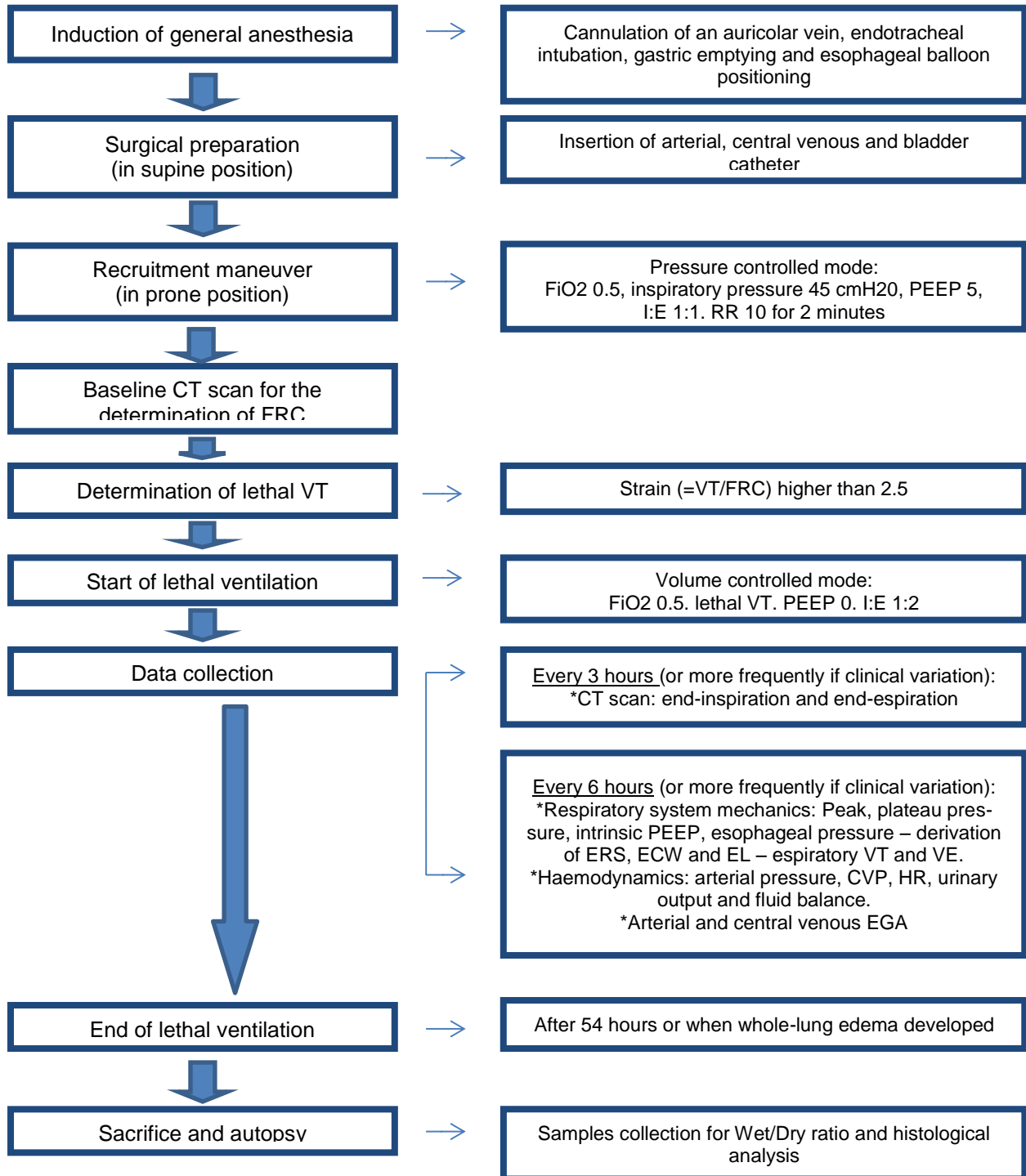
Supplemental Digital Content 1

Massimo Cressoni M.D., Chiara Chiurazzi M.D., Miriam Gotti M.D., Martina Amini M.D., Matteo Brioni M.D., Ilaria Algieri M.D., Antonio Cammaroto M.D., Cristina Rovati M.D., Dario Massari M.D., Caterina Bacile di Castiglione M.D., Klodiana Nikolla M.D., Claudia Montaruli M.D., Marco Lazzerini M.D., Daniele Dondossola M.D., Angelo Colombo M.D., Stefano Gatti M.D., Vincenza Valerio PhD., Nicoletta Gagliano PhD., Eleonora Carlesso MSc, Luciano Gattinoni M.D. F.R.C.P.

Additional Methods

Study design

Figure 1 – Flowchart of the study



Anesthesia and surgical preparation

Anesthesia was induced with an intramuscular injection of medetomidine 0.025 mg/kg and tiletamine/zolazepam 5 mg/kg. An auricular vein was cannulated. The animal was kept in prone position and, after preoxygenation, an endotracheal tube was inserted in prone position and mechanical ventilation started. Anesthesia was maintained with propofol 5-10 mg/kg/h, pancuronium bromide 0.3-0.5 mg/kg/h and medetomidine 2.5-10.0 µg/kg/h. Normal saline (NaCl 0.9%) was administered at 100 ml/h during surgery and 50 ml/h thereafter. Ceftriaxone 1 g i.v. and Tramadol 50 mg i.v. were administered preoperatively and every 12 hours thereafter. Low molecular weight heparin 2000 IU was given subcutaneously once a day.

Surgical preparation was carried out under sterile conditions, with piglets under general anesthesia and in supine position. During the procedure, mechanical ventilation was set as follows:

- Volume-controlled mode
- Fraction of inspired oxygen (FiO_2) = 0.5
- Tidal Volume (V_T) = 10 ml/kg
- Respiratory rate (RR) = 20-22 breaths per minute
- Positive end-expiratory pressure (PEEP) = 3-5 cmH₂O
- Inspiratory to expiratory time ratio (I:E) = 1:2

Right carotid artery was exposed and cannulated. A three lumen central venous catheter was inserted through the right internal jugular vein. A bladder catheter was positioned via cystostomy. Once the surgical procedure was completed, the animal was turned prone. Stomach emptying was performed by gastric suction. A latex thin wall, 5 cm long, esophageal balloon was advanced in

the inferior third of the esophagus and filled-in with 1.5 ml of room air. Proper positioning of endovascular catheters and esophageal balloon was later verified on thorax computed tomography. Pressure transducers were connected to the endotracheal tube, the esophageal balloon and the endovascular catheters, zeroed at room air at heart level, as appropriate. Data were recorded and analyzed using a dedicated software (Colligo, Italy, www.elekton.it).

Lung computed tomography

Before the beginning of the study, a baseline CT scan (Lightspeed, General Electric) was obtained. Each piglet underwent a recruitment maneuver, defined as two minutes of pressure-controlled ventilation with the following settings:

- $FiO_2 = 0.5$
- Inspiratory pressure = 45 cmH₂O
- RR = 10 breaths per minute
- PEEP = 5 cmH₂O
- I:E = 1:1

Lung CT scan was performed with the following settings:

- Collimation width: 32 x 2 x 0.6 mm
- Spiral pitch factor: 1.2
- Slice thickness: 5 mm
- Reconstruction interval: 5 mm
- Data collection FOV: 500 mm

- Reconstruction FOV: 300 mm
- KVp: 120
- X-Ray Tube Current: 110 mA
- Pixel dimensions: 0.585938/0.585938
- Acquisition matrix: 512 x 512

Study ventilatory settings

Volume-controlled mechanical ventilation was set as follows:

- $FiO_2 = 0.5$
- V_T corresponding to a strain (V_T/FRC , see above) greater than 2.5, which corresponds to 750 ml in piglets of about 20-25 Kg, or to 38-40 ml/Kg.
- Respiratory rate = 15 breaths per minute
- PEEP = 0 cmH₂O
- I:E = 1:2

Strain was defined as the ratio between V_T and functional residual capacity (FRC). The value of 2.5 was chosen because it is known to be lethal within 54 hours¹. The animals were ventilated with no PEEP in order to avoid any of its potential protective effects and to facilitate the onset of lung lesions.

Hemodynamic protocol

To maintain hemodynamic stability, a target mean arterial pressure (MAP) was set between 60 and 70 mmHg, with continuous saline infusion (50 ml/h). A fall in MAP below 60

mmHg was corrected with saline bolus (100-150 ml) and increases in saline infusion, up to 75-100 ml/h. If these were not sufficient to restore the target MAP, norepinephrine was administered, from a minimum of 0.1 µg/kg/min to a maximum of 1.0 µg/kg/min. If MAP rose above 70 mmHg, hemodynamic support was deescalated. Cumulative fluid intake was computed as the sum of intravenous fluids infused but not including drugs. Fluid balance was computed as cumulative fluid intake minus total urinary output.

Data collection

A complete data collection was performed at least every 3 hours or more often if respiratory or hemodynamic variables changed. Prior to data collection, tracheal suctioning was performed. V_T , airways pressure (Paw) and esophageal pressure (Pes) were recorded during end-inspiratory and end-expiratory pauses.

Transpulmonary pressure was computed at end-inspiration as:

$$\Delta\text{Transpulmonary pressure (cmH}_2\text{O)} = \Delta\text{Airway pressure (cmH}_2\text{O)} - \Delta\text{esophageal pressure (cmH}_2\text{O)}$$

$$\Delta\text{Airway pressure (cmH}_2\text{O)} = \text{Plateau airway pressure (cmH}_2\text{O)} - \text{End expiratory pause airway pressure (cmH}_2\text{O)}$$

$$\Delta\text{Esophageal pressure (cmH}_2\text{O)} = \text{Plateau esophageal pressure (cmH}_2\text{O)} - \text{End expiratory pause esophageal pressure (cmH}_2\text{O)}$$

Plateau airway and esophageal pressure were measured during an end-inspiratory pause.

Respiratory system (E_{RS}), lung (E_L) and chest wall (E_{CW}) elastance were calculated:

$$E_{RS} = \Delta P_{aw} / V_T$$

$$E_L = \Delta(P_{aw} - P_{es}) / V_T = \Delta P_L / V_T$$

$$E_{CW} = \Delta P_{es} / V_T$$

ΔP_L and ΔP_{es} were defined as the difference between end-inspiratory (plateau) and end-expiratory transpulmonary and esophageal pressures, respectively. Arterial and central venous blood gases were analyzed (ABL825FLEX, Radiometer, Copenhagen, Denmark[®]). Variables describing systemic hemodynamics were recorded; central venous pressure (CVP) was measured during an end-expiratory pause. Urine output was recorded and fluid balance over a 6 hours period was calculated. Rectal temperature was measured. Every 3 hours, 2 CT scans were performed. The former was obtained during an end-inspiratory pause, the latter during an end-expiratory pause.

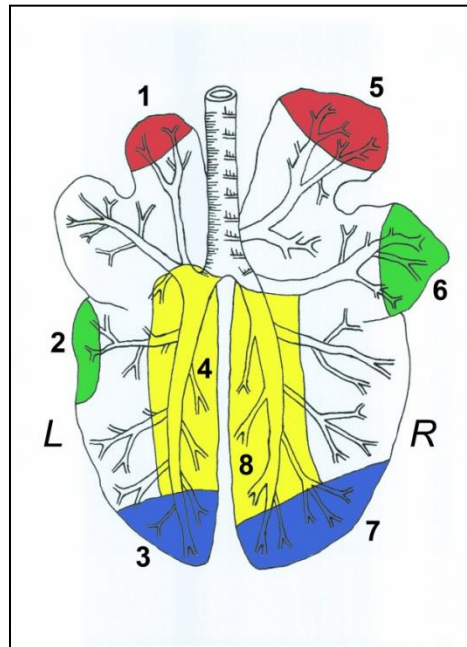
Sacrifice and autopsy

After the scheduled 54 hours of the study, or before if whole lung edema developed, piglets were sacrificed with a bolus injection of KCl 40 mEq i.v. under deep sedation, obtained with a 50 mg bolus dose of propofol. After sacrifice, tracheal tube was clamped during end-inspiratory pause. Chest was opened and trachea was clamped and cut. Lungs were excised and weighed, keeping the trachea clamped.

Light microscopy

Each lung was divided in 4 regions, as shown in Figure 2.

Figure 2: Lung regions for histological samples



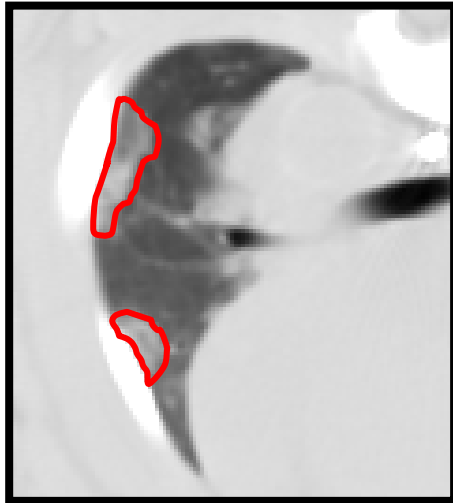
Lung fragments were obtained from each region of both lungs: three samples from subpleural regions taken at the tips of the lobes (1, 2, 3, 5, 6, 7 in Figure 2) and one sample from the internal part of the lung (4, 8 in Figure 2). Fragments were immediately processed for morphological procedures by fixation in 4% formalin in 0.1M phosphate buffered saline (PBS), pH 7.4. After fixation lung fragments were routinely dehydrated, paraffin embedded, and serially cut (thickness 5 μ m). For each specimen and for each staining we analysed three slides obtained at a 100 μ m distance. Sections were stained with freshly made hematoxylin-eosin to evaluate cells and tissue morphology. To obtain specific stain for fibrillary collagen, sections were deparaffinised and immersed for 30 minutes in saturated aqueous picric acid containing 0.1% Sirius red F3BA (Sigma, Milan, Italy)². To analyze elastic fibers, sections were stained in blue-black by Weigert's resorcin-fuchsin^{3,4}. Briefly, after bringing sections to water, they were incubated for 2 minutes in potassium permanganate, washed in water and immersed in 1% Oxalic acid for 1 minute. After washing, slides were stained o.n. in Weigert's resorcin-fuchsin at room

temperature. Hematoxylin-eosin stained sections for each lung region were analysed at light microscope in blind by two independent operators using a semi quantitative grading scale to assess various features of the tissue. The variables included in the scale for the analysis of lung structure and damage were: hyaline membranes formation, diffusion and severity of interstitial and septal infiltrate, vascular congestion and intra-alveolar haemorrhaging, alveoli rupturing and basophilic material deposition. Overall injury was expressed by a scoring system from 0 to 4: 0 - no alterations, 1 - 25% of field involved; 2 - 50 % of field involved; 3 - 75 % of field involved; 4 - 50 100% of field involved. For elastin and collagen content analysis slides were photographed by a digital camera connected to a Nikon Eclipse 80i microscope. At least 8 fields per section per area were analyzed with Photoshop (Adobe, USA) allowing to detect resorcin-fuchsin and Sirius red stained tissue. Collagen and elastin content were expressed as a percent of the stained area relative to the lung tissue. For this purpose, we considered the effective lung parenchyma excluding the areas occupied by lung alveoli lumen, and we excluded perivascular and peribronchiolar regions.

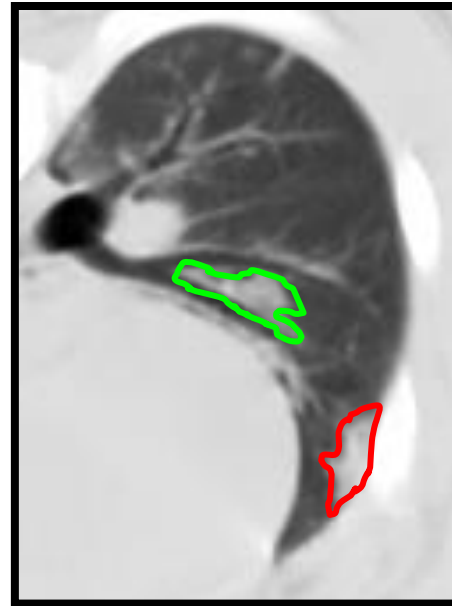
Wet to dry ratio

Three samples from each lung (upper, medium and lower lobe) were collected. They were immediately weighed and, after being dried for 24 hours at 50 °C, were weighed again. Wet to dry ratio was determined as the ratio between the two measurements.

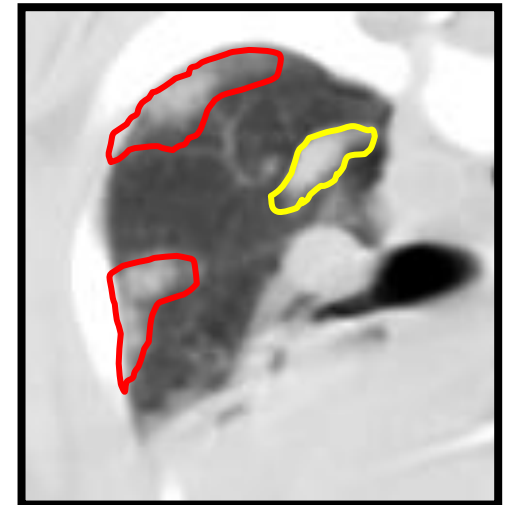
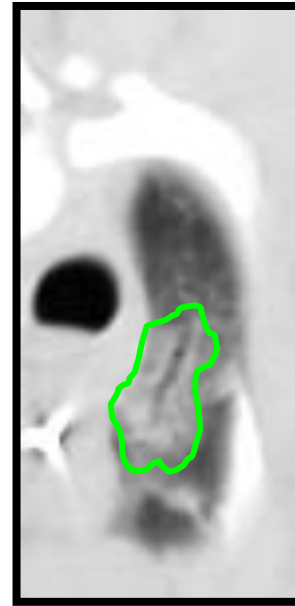
Figure 3: New densities classification



Subpleural



Peribronchial



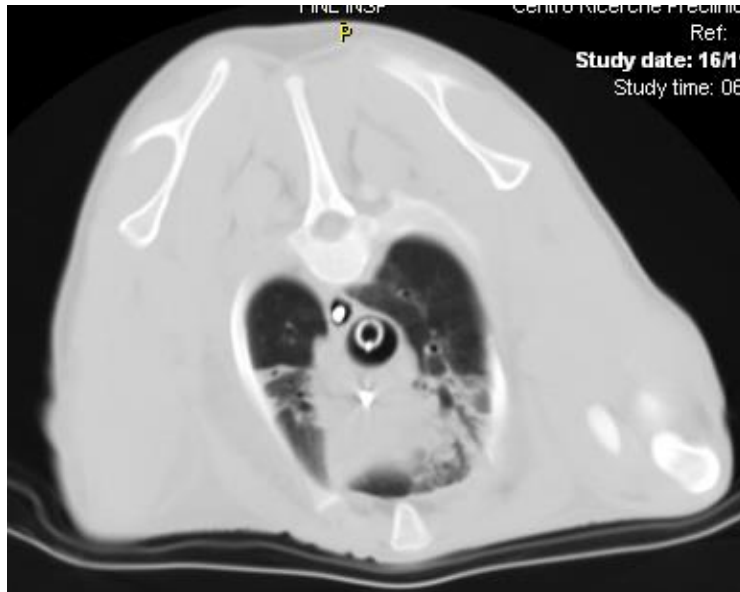
Parenchymal

New densities classified as: subpleural (red line); peribronchial (green line); parenchymal (yellow line).

CT scan: baseline lung densities

An example of an end-inspiratory density is shown in the figure below:

Figure 4



Before the beginning of the study, two CT scans were performed, the former at end-inspiration and the latter at end-expiration. A recruitment maneuver (see above) preceded the CT scan. On the basis of these scans, two groups of animals were identified: the first group included pigs with non-recruitable baseline lung lesions; the second group included pigs without pulmonary infiltrates. Baseline lesions were manually delineated and were kept delineated in end-expiration and in end-inspiration scans along the study, until whole lung edema developed.

Quantitative analysis of CT scan

For each CT scan obtained during the study, lung profiles were manually drawn. Analysis was performed using a dedicated software (SoftEFilm, Elekton, Italy, www.softefilm.eu). The density of lung parenchyma was assumed to be close to the density of water (0 HU) and each voxel was assumed

to be formed by two compartments: lung tissue (including blood, 0 HU) and air (-1000 HU).

Gas fraction was computed in each voxel as:

$$\text{Volume gas} / (\text{volume gas} + \text{volume tissue}) = \text{mean CT number observed} / (\text{CT number gas} - \text{CT number tissue})$$

Rearranging:

$$\text{Gas fraction} = \text{voxel density (Hounsfield units)} / -1000$$

$$\text{Tissue fraction} = 1 - \text{gas fraction}$$

Consequently, gas and tissue volumes can be defined as:

$$\text{Gas volume} = \text{gas fraction} \times \text{voxel volume}$$

$$\text{Tissue volume} = \text{tissue fraction} \times \text{voxel volume}$$

Voxel weight is equal to the tissue volume, assuming that tissue density is 1.

Aeration of lung parenchyma was classified in four subsets:

- Not inflated tissue: density > -100 HU
- Poorly inflated tissue: density between -100 and -500 HU
- Well inflated tissue: density between -500 and -900 HU
- Over inflated tissue: density < -900 HU

We defined “new density” a region of at least 6 mm (inner diameter of tracheal tube) of maximal diameter with a density corresponding to poorly or not inflated tissue, not present in the previous CT scan and distinguishable from the surrounding parenchyma. For seek of clarity the new densities are defined in the manuscript as “densities”. The densities were classified by 3 independent observers (M.G., C.C. and M.L.). New densities were classified on the basis of location in the lung. New

densities under the visceral pleura were classified as sub pleural; new densities near bronchi were classified as peribronchial; all the remaining densities were classified as parenchymal. New densities were also classified dividing lungs into 6 fields: dependent vs non dependent regions (lesions respectively above or under an ideal line through the trachea or the centre of the lung) and apex/hilum/basis (if new densities are respectively above the carena, between carena and diaphragm appearance and under diaphragm appearance level). Note that new densities could be classified as peribronchial only if a bronchogram was clearly identifiable, while many parenchymal new densities were located near a blood vessel but, since the vessel was not clearly identifiable without contrast medium these lesions could not be counted as “perivascular”.

Piglet lung acinus size determination

As the ratio between airway space dimensions and animal weight follows a logarithmic scale⁵ we estimated the acinar volume of piglets from the data presented by Sapoval and Weibel⁶ reporting the acinus size in mouse, rat, rabbit and humans. For humans we used the 1/8 subacinus since, as detailed by the authors, this 1/8 subacinus is more comparable to acini in other species^{E7} and computed an acinar volume of 12.1 mm³ corresponding to a radius of 1.42 mm.

Figure 5

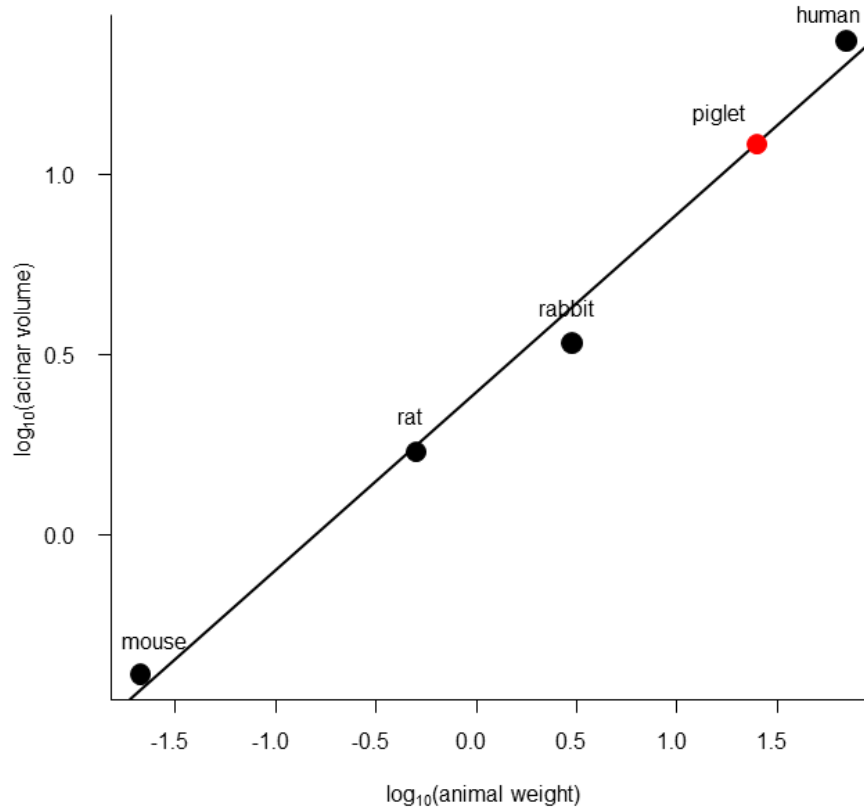


Figure 5 presents the relationship between \log_{10} of animal weight and \log_{10} of acinar volume in mouse, rat, rabbit and human as described in reference 6. For the human acinus the size of 1/8 subacinus was used. $\log_{10}(\text{acinus size}) = 0.39363 + 0.49331 \cdot \log_{10}(\text{animal weight in Kg})$, $r^2=0.99$, $p<0.01$). The computed \log_{10} of the acinar size of 25 Kg piglet is reported with a red dot.

*Lung inhomogeneities determinations*⁸

Since CT scan images are composed by voxels whose dimensions depend both on the CT scan hardware and on the setting for image reconstruction, we decided to produce a lung inhomogeneities map with dimensions 1:1 to the original CT scan map, but using as a “basic dimension” the acinar volume and filtering the map with a gaussian filter with a radius equal to the radius of the acinus. In this way, we obtained a CT value of each voxel which was dependent to the CT value of the neighboring voxels. Around each voxel we defined a spherical crust starting at distance of one acinar radius from the voxel center and of $\frac{1}{2}$ acinar radius thickness. The ratio of the surrounding voxel gas to the central voxel gas fraction indicates homogeneity if equal to 1, inhomogeneity when greater than 1. We computed a vector of lung inhomogeneities dividing the filtered gas fraction in each of the voxels included, at least partially, in the spherical crust and the filtered value of the central voxel and we wrote the maximum of the vector in the lung inhomogeneities map. It must be stressed that while average is a square filter and takes into the same account near and far voxels, gaussian filters exponentially decreases weight of far voxels. We considered as stress raisers those points causing inhomogeneities greater than 95th percentile of the values observed in our normal piglets at baseline resulting in a threshold of 1.685. Lung inhomogeneity was expressed both as intensity (average ratio) and extent (fraction of lung volume with inhomogeneities greater than 1.685). The pressure multiplication factor by the stress raiser can be estimated according to Mead et al.⁹ as the volume/gas ratio between two lung regions elevated to the 2/3 power (factor scale from volumes to surfaces).

Study time-points

In order to study the development of VILI in our piglets, we decided to synchronize our analysis establishing 6 time-points. Every time-point corresponds to a defined CT image pattern. The time-points are the following:

- *Time 0* – the baseline CT scan
- *Time 1* – the last CT scan without new densities
- *Time 2* – the first CT scan with at least a new density
- *Time 3* – the last CT scan in which the new densities were distinguishable
- *Time 4* – the first CT scan with one-field edema, that is a pattern in which increase of density occupies at least 1 lung field previously described
- *Time 5* – the first CT scan with all-field edema, that is a pattern in which increase of density occupies all the 6 lung field previously described

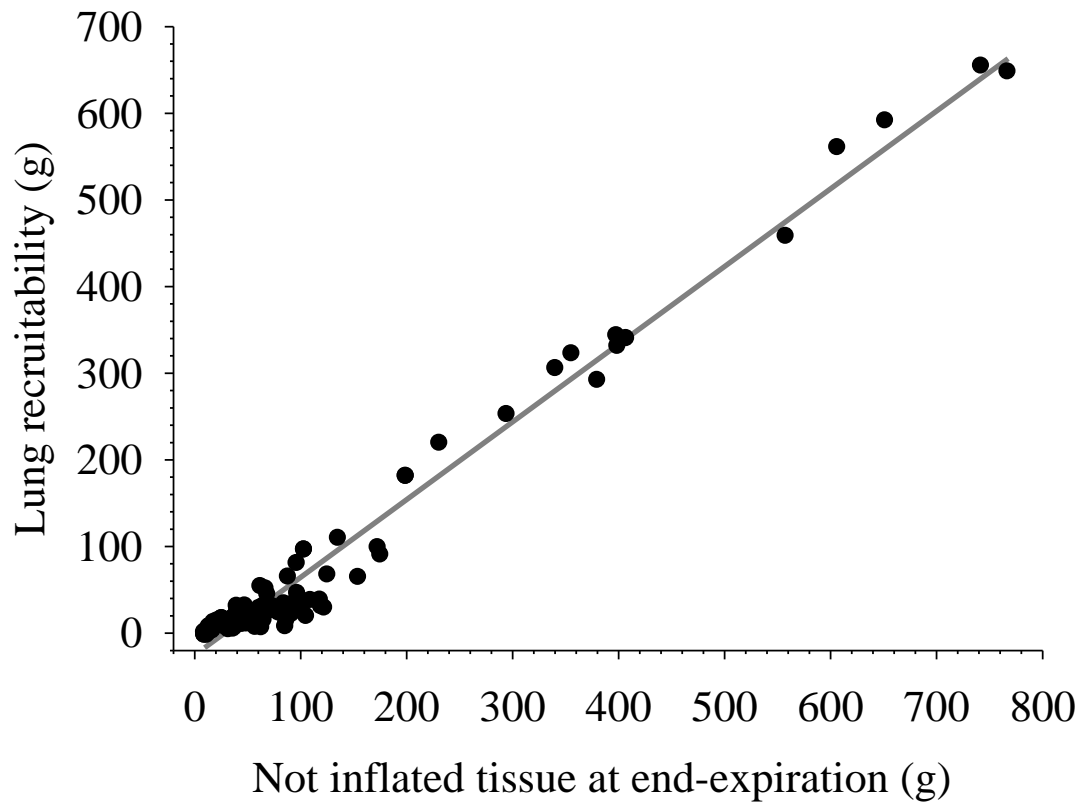
In 5 piglets some of the above time-points were coincident, because of a rapid evolution of CT scan pattern (see Table 1). As shown, this phenomenon occurred mainly in piglets with baseline lesions.

Table 1

Pig code	Baseline lesions	Coincident time-points
KT	YES	T0-T1-T2-T3
RB	NO	T0-T1 and T4-T5
MN	YES	T0-T1 and T2-T3
DLC	YES	T4-T5
JNN	YES	T4-T5

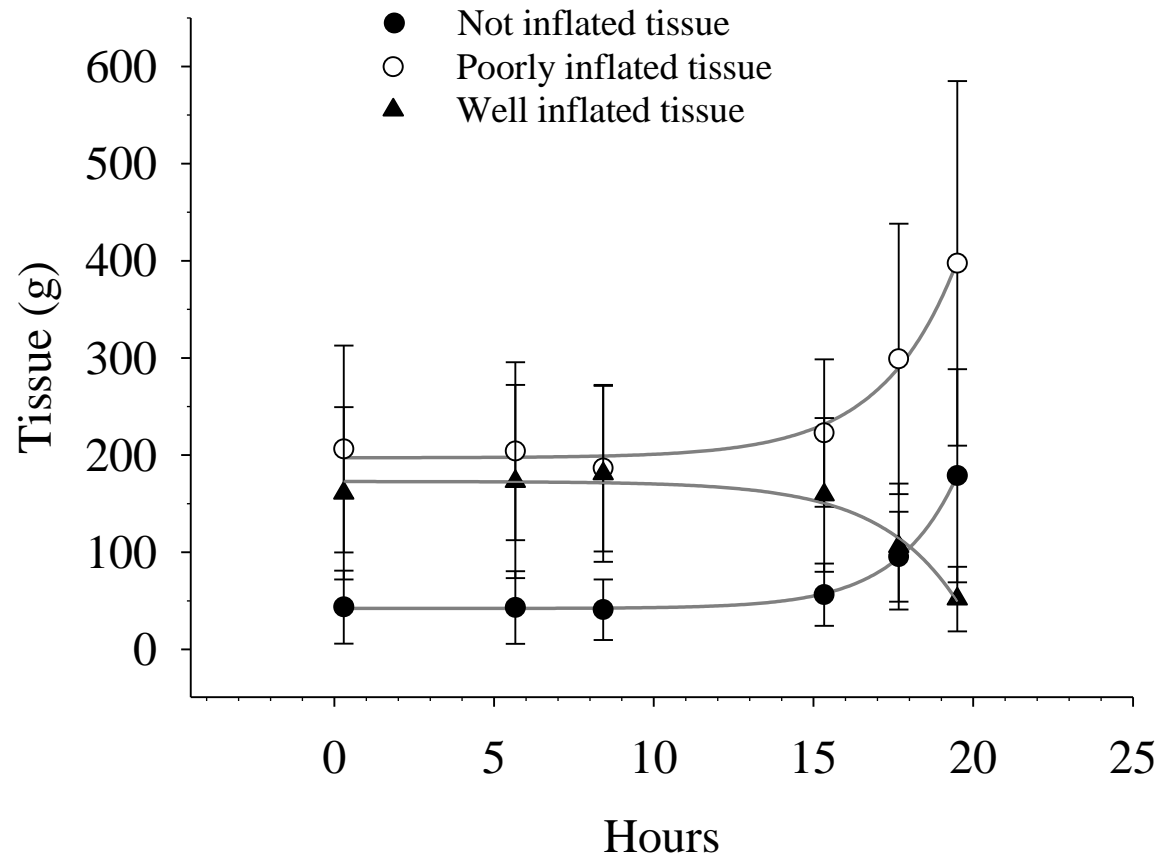
Additional results

Figure 6 – Recrutable lung tissue as function of not inflated lung tissue at end-expiration



Lung recruitability (y axis) as a function of not inflated tissue (g) at end-expiration (x axis). (Lung recruitability (g) = -25 + Not inflated tissue at end-expiration (g) * 0.90, $r^2 = 0.97$, $p < 0.0001$) .

Figure 7 – Time-course of not-inflated, poorly inflated and well-inflated tissue



Time course of not inflated (black dots), poorly inflated (white dots) and well inflated (triangles) tissue \pm SD at the 6 time points (x axis).

(Not inflated tissue (g) = $42 + 0.005 * e^{0.52 * \text{hours}}$, $r^2 = 0.99$, $p < 0.0001$;

Poorly inflated tissue (g) = $197 + 0.051 * e^{0.42 * \text{hours}}$, $r^2 = 0.99$, $p = 0.0016$;

Well inflated tissue (g) = $172 - 0.042 * e^{0.41 * \text{hours}}$, $r^2 = 0.97$, $p = 0.0054$).

Pre-study physiological variables in pigs with and without non recruitable end-inspiratory densities

Piglets with and without recruitable baseline lung densities presented similar gas exchange variable before starting the study (i.e. with a V_T of approximately 10 ml/Kg) while the E_{RS} resulted to be significantly different despite a similar plateau pressure.

Table 2 – Comparison of pre-study variables between piglets with and without baseline densities

	Piglets <u>with</u> recruitable baseline lung densities (n=6)	Piglets <u>without</u> recruitable baseline lung densities (n=6)	P value
Weight (Kg)	21±2.5	22±6.3	0.60
V_T (ml)	285±50	308±34	0.37
PaO ₂ /FiO ₂	482±82	487±106	0.92
PaCO ₂ (mmHg)	41±7.3	43±3.3	0.60
Arterial pH	7.4±0.062	7.4±0.088	0.25
Plateau pressure (cmH ₂ O)	16±3.2	15±1	0.24
E_{RS} (cmH ₂ O/l)	58±5.2	48±6	0.01
Mean arterial pressure (mmHg)	78±8.8	82±9.3	0.57
Heart rate (beats/min)	77±16	96±18	0.15
CVP (mmHg)	6.5±5	7.5±5.7	0.78
ScvO ₂ (%)	78±8.8	82±9.3	0.57

Blood gas and hemodynamic variables were compared with unpaired t-test.

Pre-study CT-scan variables in piglets with and without non recruitable end-inspiratory densities

CT scan data showed a trend toward increased total lung weight, increased fraction of not inflated tissue and a trend toward a reduced fraction of well inflated tissue and significantly greater lung inhomogeneities extent. The total volume of baseline lesions was 61 ± 54 ml and their average CT number was -115 ± 77 HU. Note that the lung inhomogeneities extent is computed on the pre-study CT scan and is different from the Baseline one reported in Table 2, which is recorded after starting the study.

Table 3 – Comparison of pre-study variables between piglets with and without baseline densities

	Pigs <u>with</u> recruitable baseline lung densities (n=6)	Pigs <u>without</u> recruitable baseline lung densities (n=6)	P value
Total tissue (g)	459±65	361±83	0.06
Total gas (g)	333±98	405±132	0.34
Not inflated tissue (%)	15±6.2	5±2.5	0.01
Poorly inflated tissue (%)	56±20	40±22	0.23
Well inflated tissue (%)	29±23	55±22	0.08
Over inflated tissue (%)	0.0083±0.0053	0.032±0.023	0.06
Extent of lung inhomogeneities (% of lung volume)	9.6±3.9	5.2±1.8	0.03
Average lung inhomogeneities	2.5±0.22	2.6±0.28	0.48

CT-scan variables were compared with unpaired t-test.

Length of mechanical ventilation

Piglets with baseline densities tended to deteriorate more rapidly than piglets without baseline densities.

Table 4 – Comparison of length of mechanical ventilation in piglets with and without baseline densities

	Pigs <u>with</u> recruitable baseline lung densities (n=6)	Pigs <u>without</u> recruitable baseline lung densities (n=6)	P value
Time 1 (hours)	4.3±4.3	7±8.3	0.50
Time 2 (hours)	6.8±5.4	10±7.1	0.41
Time 3 (hours)	10±8.4	20±13	0.13
Time 4 (hours)	13±7.6	22±13	0.18
Time 5 (hours)	15±6.9	24±13	0.15

Times were compared with unpaired t-test.

Microscopic anatomy

Figure 8 - Microphotographs of lung sections stained with Sirius red for collagen

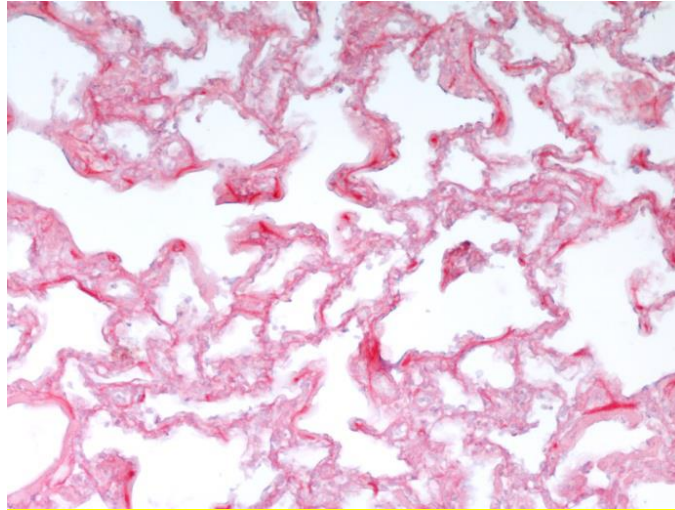
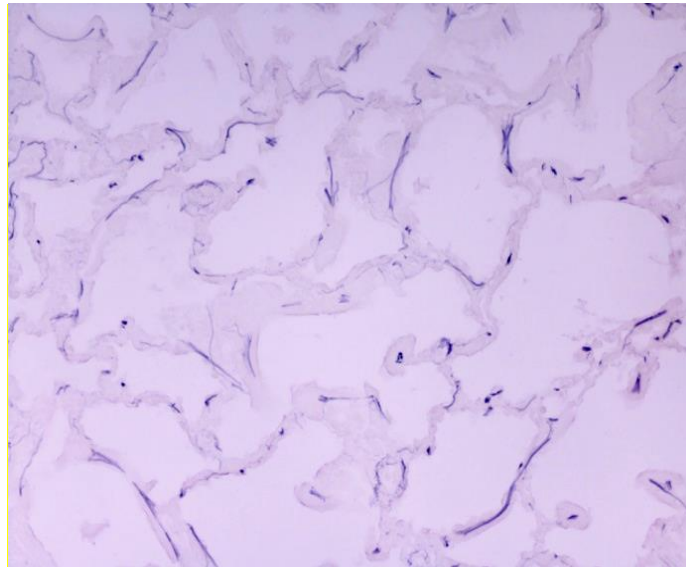


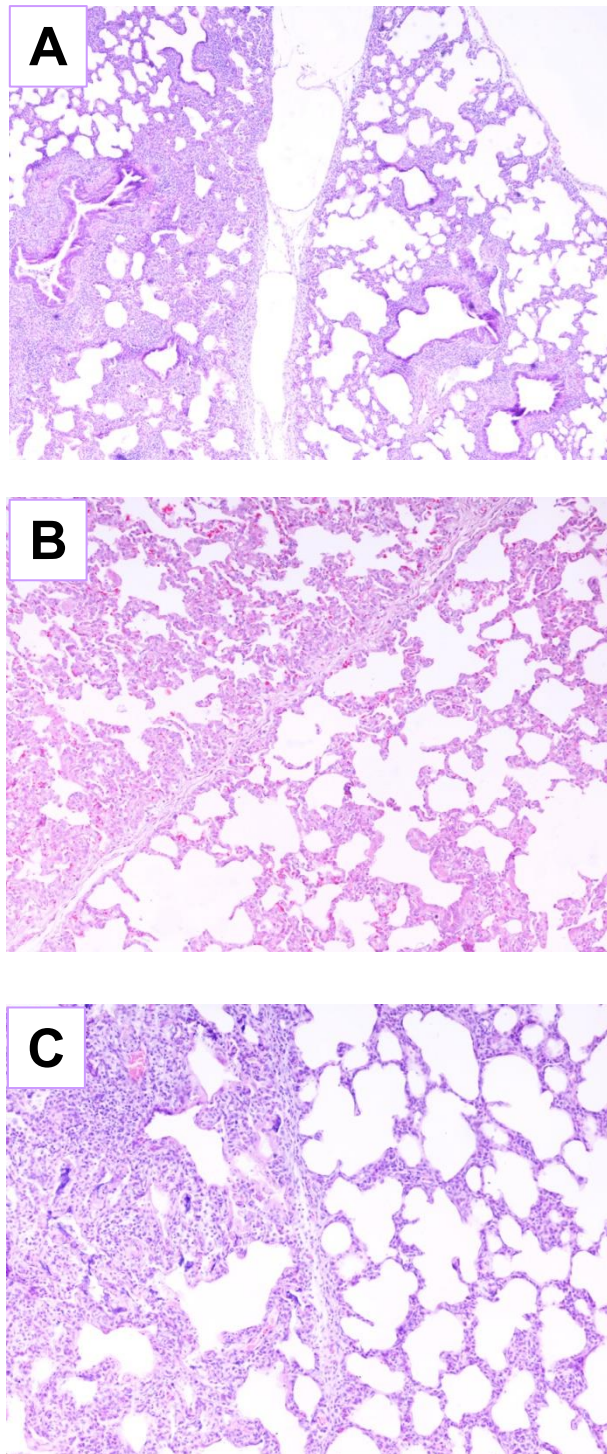
Figure 9 - Microphotographs of lung sections stained with Weigert's resorcin-fuchsin for elastin



Histological analysis were available in 7 pigs. Figure 8 shows a representative coloration of collagen and Figure 9 shows a representative coloration of elastin. The percentage of lung parenchyma

which stained for elastin was greater than the one which stained for collagen (9.45% [6.43 – 13.47] for elastin vs 4.58% [2.89 – 7.11] for collagen, $p < 0.0001$). When the fraction of parenchyma which stained for elastin were compared between the peripheral and central lung regions, no significant difference was found (median 9.45% [6.93 – 15.51] of lung parenchyma in the central regions vs 8.89% [7.52 – 10.78] in the peripheral lung regions compared to the central lung regions, $p = 0.22$); while we found a slightly greater area of stained with collagen in the peripheral lung regions compared to the central ones (median 3.80% [3.14 – 5.35] of lung parenchyma in the central regions compared to 4.48% [3.58 – 6.60] of lung parenchyma in the peripheral ones, $p = 0.047$).

Figure 10 - Microphotographs showing lung sections stained with Hematoxylin-Eosin



Microphotographs showing lung sections stained with H&E. Lung damage ranged from moderate to severe. Panel B shows the presence of a connective septum which separates, in the same field, two

different diseases presentation. Original magnification: 4x (A), 10x (B, C). We observed, within the parenchyma, septa of connective tissue, which delimit the different area of damage (ranging from moderate to severe). We may speculate that also those intrinsic inhomogeneities of parenchyma could act as pressure multipliers. However, this is an anatomical feature of the animal in question, which then finds no analogy with the ultra structural features of the human lung.

Figure 11 – Ratio between intra and extra-alveolar infiltrate

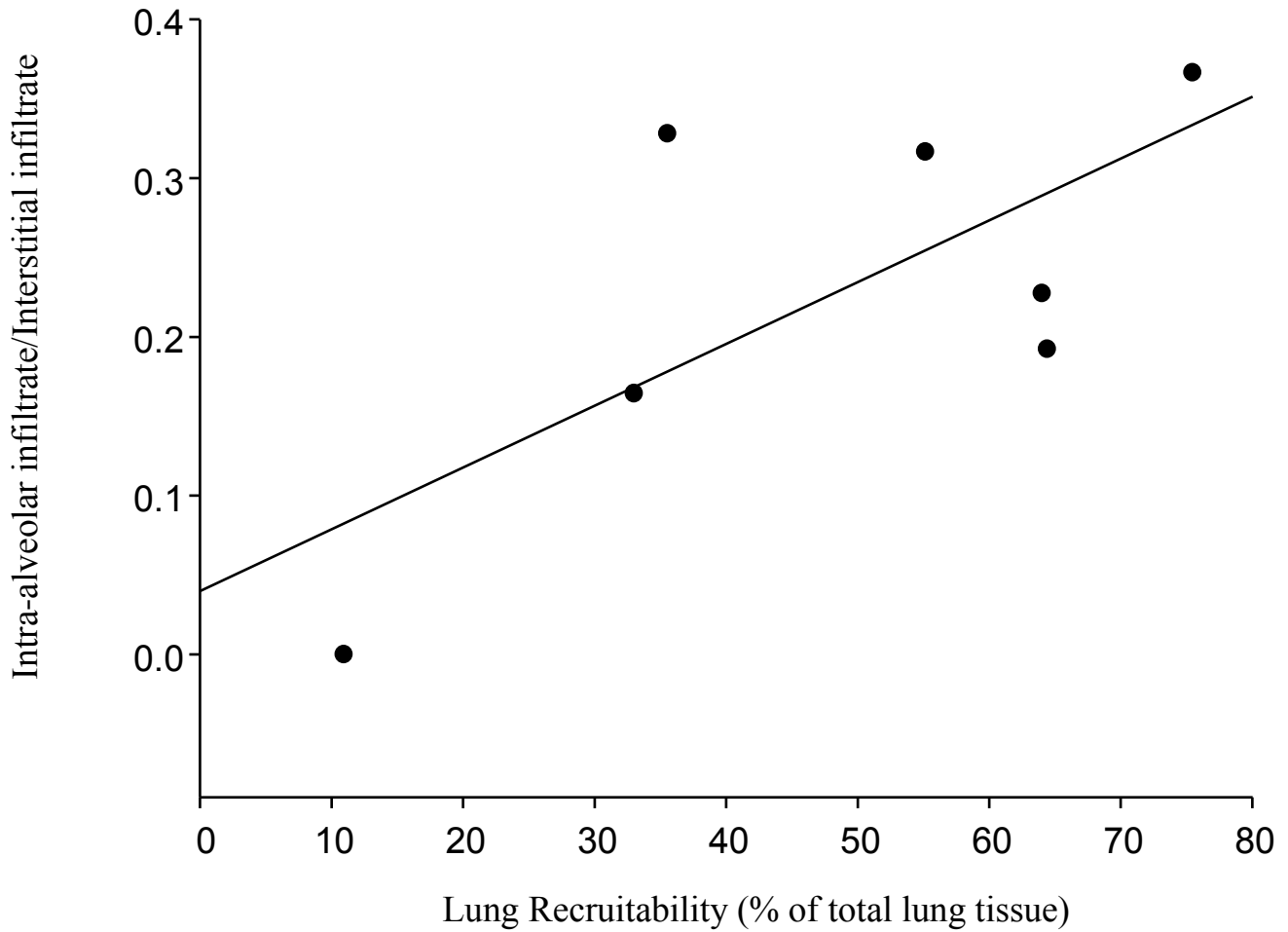


Figure presents the ratio of intra to extra-alveolar infiltrate as a function of lung recruitability. Lung recruitability (% of total tissue) = $0.194 + 1.271 * \text{Intralveolar/Extralveolar, infiltrate ratio}$, $r^2 = 0.5$, $p=0.07$

Table 5 – Dependent/non dependent distribution of new densities

	Non Dependent	Dependent	P value
Subpleural	9 [4.75 - 14]	5 [2.75 - 12.00]	
Parenchymal	1 [0 - 3.25]	4 [1.5 - 7]	
Peribronchial	1 [0 - 3.25]	4 [0.75 - 5.25]	
Total	12 [5.50- 20.75]	15.5 [7.25 - 24.75]	0.11

Table summarizes the number of new densities in the dependent and non dependent lung regions expressed as median – interquartile range. The total number of new lesions was analyzed with a mixed model on the ranked number of lesions using as fixed effects the density localization (subpleural/parenchymal/peribronchial) and the spatial localization as dependent/non dependent and apex/hilum/base. The subpleural/parenchymal/peribronchial localization was highly significant ($p < 0.0001$) as it was the apex/hilum/base localization while the dependent/non dependent localization was not significant ($p = 0.11$), but the interaction term between subpleural/parenchymal/peribronchial was significant ($p = 0.0057$); the other interaction terms were not significant.

Table 6 – Hemodynamic variables

	Baseline CT-scan (Time 0)	Last CT-scan without new densities (Time 1)	First CT-scan with new densities (Time 2)	Last CT-scan with distinguishable densities (Time 3)	First CT-scan with one-field edema (Time 4)	First CT-scan with all-field edema (Time 5)	P value
Time (hours)	0±0	5.7±6.5	8.4±6.3	15±12	18±11	20±11	
Mean Arterial Pressure (mmHg)	92±19	87±17	93±16	87±22	81±23	82±25	0.34
Central Venous Pressure (mmHg)	6.3±4.5	6.6±4	7.3±3.6	7.3±3.6	8±3.3	8.1±4.1	0.10
SvO ₂ (%)	75±14	70±13	65±11*	63±8.2*	59±12*	52±14*	<0.001
Arterial-venous oxygen difference (ml/dl)	4±1.6	4.6±1.7	5.3±1.3	5.4±1.2*	5.7±1.2*	7.1±2.3*	<0.01
Arterial lactates (mmol/l)	1.9±1	1.9±1.1	1.8±1.1	1.6±0.94	1.4±0.78	2.2±1.6	0.39
Cumulative fluid intake (ml)	1358±790	2134±1753	2451±1694*	3425±2312*	3812±2293*	4087±2382*	<0.0001
Cumulative urinary output (ml)	788±823	1254±1283	1600±1301*	2451±1564*	2669±1556*	3091±2064*	<0.0001
Cumulative fluid balance (ml)	570±507	880±730	851±720	974±974	1143±1109	996±1032	0.10
Vasopressors (number of pigs/total number of pigs)	0/12	0/12	0/12	2/12	2/12	5/12	0.06 †

* p < 0.05 vs baseline (Time 0) † Fisher's exact test.

Figure 12

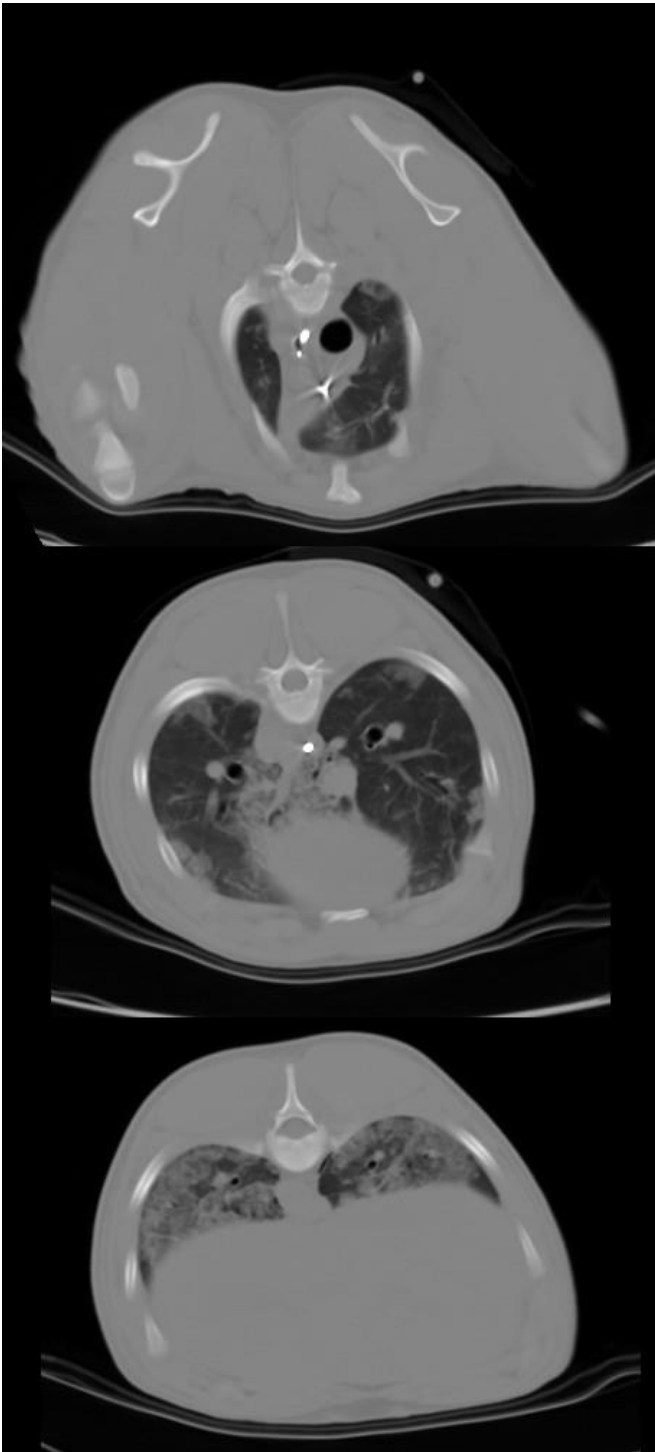


Figure 12 presents a CT scan taken at Time 4 with three images showing the 6 lung fields (apex dependent/non dependent, hilum dependent/non dependent and base dependent/non dependent). As shown at the basis lung fields are not inflated.

Reference List

1. Protti A, Cressoni M, Santini A, Langer T, Mietto C, Febres D, Chierichetti M, Coppola S, Conte G, Gatti S, Leopardi O, Masson S, Lombardi L, Lazzerini M, Rampoldi E, Cadringer P, Gattinoni L: Lung stress and strain during mechanical ventilation: any safe threshold? *Am J Respir.Crit Care Med* 2011; 183: 1354-62
2. Junqueira LC, Bignolas G, Brentani RR: Picrosirius staining plus polarization microscopy, a specific method for collagen detection in tissue sections. *Histochem.J* 1979; 11: 447-55
3. Rosenquist TH: Organization of collagen in the human pulmonary alveolar wall. *Anat.Rec.* 1981; 200: 447-59
4. Rosenquist T: Improved visualization of oxytalan fibers with resorcin fuchsin. *Basic Appl.Histochem.* 1981; 25: 129-32
5. TENNEY SM, REMMERS JE: Comparative quantitative morphology of the mammalian lung: diffusing area. *Nature* 1963; 197: 54-6
6. Sapoval B, Filoche M, Weibel ER: Smaller is better--but not too small: a physical scale for the design of the mammalian pulmonary acinus. *Proc.Natl.Acad.Sci.U.S A* 2002; 99: 10411-6
7. Rodriguez M, Bur S, Favre A, Weibel ER: Pulmonary acinus: geometry and morphometry of the peripheral airway system in rat and rabbit. *Am J Anat.* 1987; 180: 143-55
8. Cressoni M, Cadringer P, Chiurazzi C, Amini M, Gallazzi E, Marino A, Brioni M, Carlesso E, Chiumello D, Quintel M, Bugeo G, Gattinoni L: Lung inhomogeneity in patients with acute respiratory distress syndrome. *Am J Respir.Crit Care Med* 2014; 189: 149-58
9. Mead J, Takishima T, Leith D: Stress distribution in lungs: a model of pulmonary elasticity. *J Appl.Physiol* 1970; 28: 596-608